ACS Medicinal Chemistry Letters

Letter

pubs.acs.org/acsmedchemlett

Photoinduced Conversion of Antimelanoma Agent Dabrafenib to a Novel Fluorescent BRAF^{V600E} Inhibitor

Boris Pinchuk, Thorsten von Drathen, Viktoria Opel, and Christian Peifer*

Institute of Pharmacy, University of Kiel, Gutenbergstr. 76, D-24118 Kiel, Germany

Supporting Information

ABSTRACT: Dabrafenib (Tafinlar) was approved in 2013 by the FDA as a selective single agent treatment for patients with BRAF^{V600E} mutation-positive advanced melanoma. One year later, a combination of dabrafenib and trametinib was used for treatment of BRAF$^{V600E/K}$ mutant metastatic melanoma. In the present study, we report on hitherto not described photosensitivity of dabrafenib both in organic and aqueous media. The half-lives for dabrafenib degradation were determined. Moreover, we revealed photoinduced chemical conversion of dabrafenib to its planar fluorescent derivative dabrafenib_photo **2**. This novel compound could be isolated and biologically characterized *in vitro*. Both enzymatic and cellular assays proved that **2** is still a potent BRAF^{V600E} inhibitor. The intracellular formation of **2** from dabrafenib upon ultraviolet irradiation is shown. The herein presented findings should be taken in account when handling dabrafenib both in preclinical research and in clinical applications.

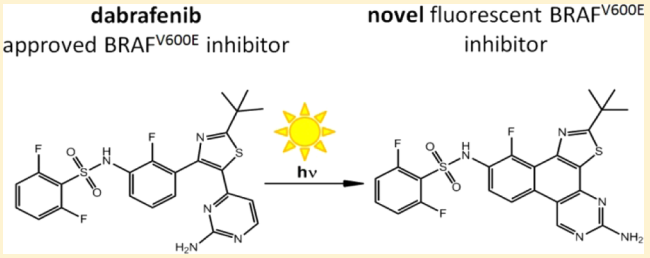

KEYWORDS: *Dabrafenib, BRAF^{V600E}, photoinduced conversion, kinase inhibitor, fluorescent probe*

Dabrafenib was the second selective BRAF^{V600E} inhibitor after vemurafenib that was approved for the treatment of BRAF^{V600} mutated melanoma.[1,2] It showed significant clinical benefits compared to alkylating chemotherapeutic agent dacarbazine in clinical studies.[3] The median progression free survival (PFS) for patients treated by dabrafenib is about five months. Unfortunately, almost all patients suffer from relapses due to acquired resistance after half a year.[4] To overcome the resistance development, combined therapy targeting different kinases in the MAPK signaling pathway was proposed. Accordingly, the combination of dabrafenib and trametinib (MEK inhibitor) showed improved clinical efficacy compared to dabrafenib monotherapy in clinical trials.[5] The median PFS could be increased to 9 months. Based on this data the combination regimen of dabrafenib with trametinib was approved in 2014 by FDA.[6] Despite superior response rates and longer therapeutic benefits of the combination therapy, most patients still relapse within one year.[7] Therefore, the acquired resistance and partially severe side effects during the BRAF^{V600E}–inhibitor therapy require further research and developments in the melanoma field.

In the course of our research on photoactivatable kinase inhibitors,[8−10] we set out to design and synthesize photoprotected prodrugs of dabrafenib. A photostable parent compound is a fundamental requirement for successful caging approach. Thus, to prove the photostability of dabrafenib we irradiated 200 μM solution of the inhibitor in DMSO with 226 W/m^2 ultraviolet light (UV) at 365 nm. To our surprise, dabrafenib was not stable under the described conditions forming a number of decay products. We examined the time dependency of the photoinduced degradation and performed HPLC measurements of irradiated samples. As shown in Figure 1, the degradation is a first-order reaction with a half-life for dabrafenib of 65.0 s. Interestingly, parallel to decomposition of dabrafenib formation of a major new compound was observed

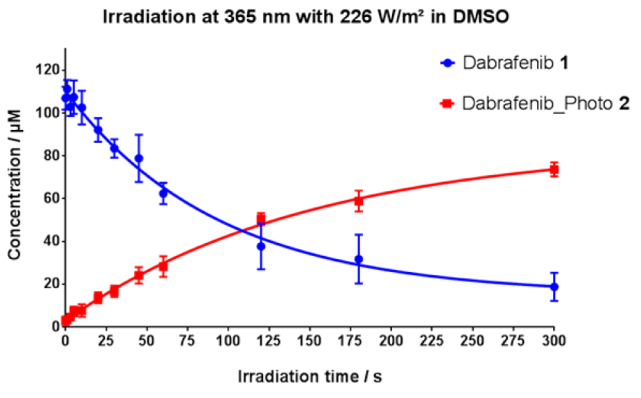

Figure 1. Photoinduced conversion of dabrafenib (**1**) to "dabrafenib_photo" (**2**). A 200 μM solution of **1** in DMSO was irradiated at 365 nm with 226 W/m^2 for up to 5 min. The irradiated samples were diluted 1:2 with methanol and analyzed by HPLC. The determined areas under the HPLC peaks were converted to appropriate compound concentrations based on calibration curves (Supplementary Figure S1) (n = 4).

Received: August 24, 2016
Accepted: September 20, 2016
Published: September 20, 2016

DOI: 10.1021/acsmedchemlett.6b00340
ACS Med. Chem. Lett. 2016, 7, 962−966

(red line in Figure 1). Accordingly to the experimental setup, we named this substance "dabrafenib_photo" (**2**).

Next, we isolated compound **2** and characterized it as *N*-(5-amino-2-(*tert*-butyl)-11-fluorobenzo[*f*]thiazolo[4,5-*h*]-quinazolin-10-yl)-2,6-difluorobenzenesulfonamide (Scheme 1).

Scheme 1. Photoinduced Conversion of Dabrafenib (1) to Dabrafenib_photo (2)

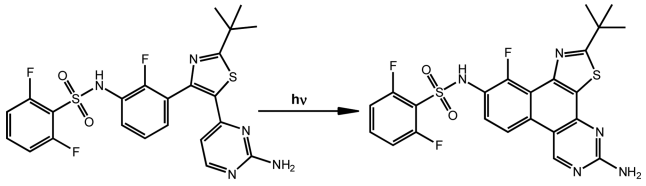

Therefore, we postulated the photoinduced conversion of dabrafenib (**1**) to the novel compound **2** in the sense of a 6-π-photocyclization followed by oxidation as described in Scheme 1.

It is noteworthy to mention that under the conditions used in our experiments the photoinduced conversion of dabrafenib (**1**) to **2** in DMSO solution is not a quantitative reaction. In line with this notion, small amounts of not further characterized byproducts were detected by HPLC analysis.

As kinase inhibitors were typically used in *in vitro* assays we next investigated whether the photoinduced degradation of dabrafenib (**1**) and the formation of **2** occurs in aqueous media too. Thus, we repeated the experiment described before but now the dabrafenib solution was prepared in cell culture medium DMEM instead of pure DMSO. When irradiated under the previously described settings the photoreaction (Scheme 1) proceeded only by approximately 10% (Supplementary Figure S2a). However, when the radiation power was increased to 1130 W/m^2 significant conversion of dabrafenib (**1**) to **2** could be detected (Supplementary Figure S2b, half-live of the dabrafenib decay was 294 s). A similar photoinduced reaction was also observed in phosphate buffered saline DPBS (Supplementary Figure S3a). Herein, the half-life of dabrafenib in DPBS was 145 s when irradiated with 1130 W/m^2 at 365 nm. Interestingly, in DMSO dabrafenib decayed significantly more readily than in aqueous solutions: half-life of **1** in DMSO was 19.5 s at 365 nm illumination by 1130 W/m^2. Moreover, the nascent **2** was not stable in DMSO under this high irradiation power and photolyzed further to several not identified products (Supplementary Figure S3b). The determined values for half-lives in different solutions are summarized in Supplementary Table S1.

Motivated by these results, we became interested in the fate of dabrafenib in aqueous solution under normal lab conditions. Indeed, under daylight exposure dabrafenib reacted relatively fast both in DMSO and in DMEM (Supplementary Figures S4 and S5). Especially in DMSO the degradation proceeded within the range of minutes and the solution became yellowish due to formation of dabrafenib_photo (**2**). In contrast to the described photoinduced conversion, we found no evidence for thermal decomposition of dabrafenib at 37 °C in the dark (Supplementary Figure S6).

The presented results are highly relevant when handling dabrafenib solutions in the lab. As consequence all dabrafenib solutions should be protected from light exposure. To our best knowledge the revealed photoinduced degradation of dabrafenib (**1**) has not been described previously. Interestingly, the CHMP (Committee for Medicinal Products for Human Use) assessment report states "...the drug substance manufactured by the proposed supplier is sufficiently stable...".[11]

Having the photoconverted product **2** in hand, we wanted to examine the photochemical properties and the biological activities of this novel compound in more detail. Accordingly, we synthesized dabrafenib_photo (**2**) in larger quantities and characterized it both photochemically and *in vitro*.

Dabrafenib_photo (**2**) reveals different spectroscopic characteristics than the parent dabrafenib (**1**). The UV/vis spectra of the compounds show increased absorption of **2** around 400 nm in comparison to **1** (Supplementary Figure S7). The bathochromic shift can be explained by the formation of a pan-aromatic phenanthrene derivative in **2**. Interestingly, this conjugated planar ring system causes green fluorescence of **2** when excited by 375 nm (Supplementary Figure S8). Therefore, when incubating cells with dabrafenib_photo **2** its intracellular localization has been analyzed by fluorescence microscopy (see below).

To further examine the biological activity of **2** several approaches were performed. First, we assumed that **2** could be a DNA intercalator due to its planar aromatic structure. However, spectrophotometric investigation (Supplementary Figure S13) and gel electrophoresis analysis (Supplementary Figure S14) have not provided any evidence for an interaction of **2** with DNA.

Based on structural similarity to dabrafenib (**1**) we supposed that **2** could also be a Braf^{V600E} inhibitor. Molecular modeling studies predicted similar binding modes of both dabrafenib (**1**) and dabrafenib_photo (**2**) in the active site of Braf^{V600E}. The calculated 2D ligand interaction diagrams are shown in Figure 2. For the 3D binding modes, see Supplementary Figure S10.

Therefore, our modeling studies support the assumption that **2** is a BRAF^{V600E} inhibitor even though the calculated docking score (Schrödinger Glide) for dabrafenib (−15.7) is higher than for **2** (−11.7).

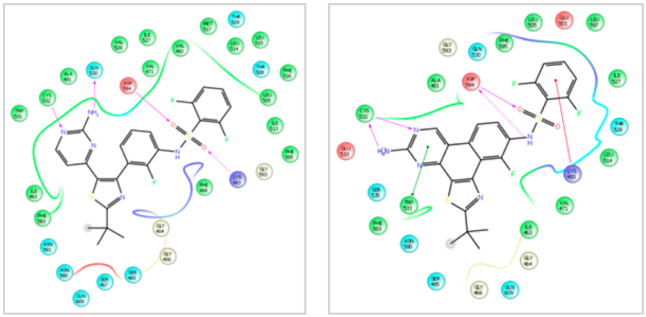

Figure 2. Modeled ligand interaction diagrams of (a) dabrafenib (**1**) and (b) dabrafenib_photo (**2**) in the active site of BRAF^{V600E} (pdb 4XV2). Key ligand−protein interactions are shown. H-bonds between the ligand and the protein backbone are indicated by purple arrows. The binding modes of both compounds are closely related: The aminopyrimidine moieties of both compounds address the hinge region of the kinase by two H-bonds. The sulfonamide residues, respectively, bind to the aspartate594 via one (**1**) or two (**2**) H-bonds. The difluorobenzene moieties occupy the deeper hydrophobic pocket I, and the *tert*-butyl residues are exposed to the solvent.

DOI: 10.1021/acsmedchemlett.6b00340
ACS Med. Chem. Lett. 2016, 7, 962−966

To prove our hypothesis, we determined the IC_{50} values of both **1** and **2** toward $BRAF^{V600E}$ (Supplementary Figure S11). In our assay the measured IC_{50} value of **1** was 9.0 nM and was thus comparable to the IC_{50} described in the literature (0.8 nM).[2,12] The IC_{50} of **2** was 280 nM. Hence, these results are in line with our modeling studies: dabrafenib_photo (**2**) is a $BRAF^{V600E}$ inhibitor although less potent than dabrafenib (**1**).

After proving the inhibitory activity of **2** toward $BRAF^{V600E}$, we set out to examine the selectivity of this compound. Thus, selectivity profiles of both **1** and **2** were measured in a panel of 321 kinases. The residual kinase activities after incubation with 1 μM compounds are displayed as TREEspot^{tm} Kinase dendrograms in Figure 3. Herein, it is obvious that **2** inhibits

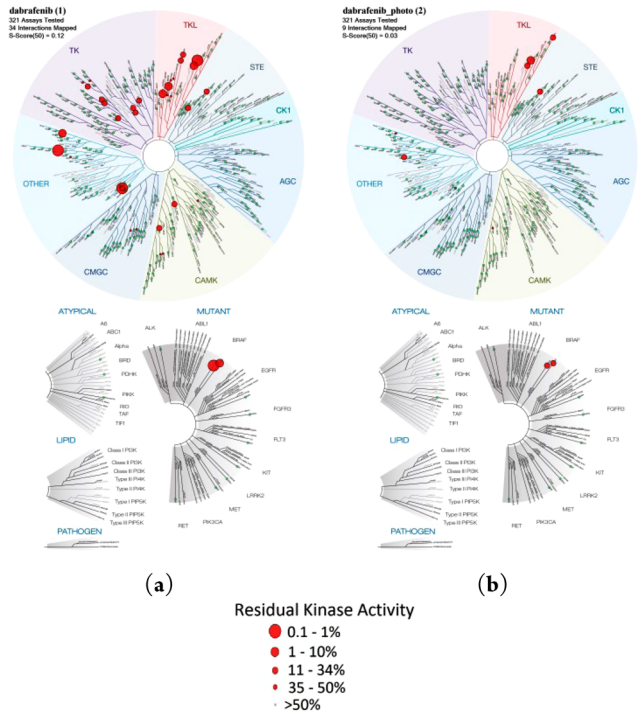

Figure 3. Dendrogram representation of the selectivity profile of compounds **1** (a) and **2** (b) at a concentration of 1 μM against 321 kinases. The residual kinase activity was determined compared to DMSO control. Images were generated using TREEspot Software Tool, DISCOVERX CORPORATION 2010. The complete raw data are shown in the Supplementary Table S2 (ProQinase, Freiburg, Germany).

significantly less kinases than **1**. Moreover, **2** has also a better selectivity score than **1** (Supplementary Table S2). Therefore, we concluded that the novel inhibitor **2** is more selective for $BRAF^{V600E}$ than dabrafenib.

Next, we examined the cytotoxic activity of **1** and **2** toward $BRAF^{V600E}$-dependent melanoma cell line SKMEL28.[13] The cellular growth was measured after 48 h incubation with different concentrations of **1** and **2**. Additionally, the first approved $BRAF^{V600E}$ inhibitor vemurafenib was included as reference. The results of these antiproliferative experiments are shown in Figure 4a.

The cellular growth assays revealed that the novel compound **2** exhibits cytostatic activity on melanoma cells in a concentration range between 10 nM and 30 μM, while at higher concentrations the effect becomes cytotoxic. The TGI-value, compound concentration at which the cell growth is

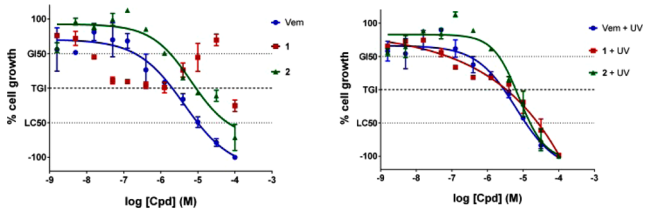

Figure 4. Antiproliferative activity of tested compounds on $BRAF^{V600E}$-dependent melanoma SKMEL28 cells. (a) Dose–response curves of dabrafenib (**1**), dabrafenib_photo (**2**), and the approved $BRAF^{V600E}$ inhibitor vemurafenib (Vem) without UV irradiation. (b) SKMEL28 cells were incubated for 1 h with the compounds and then irradiated at 365 nm (1.13 kW/m^2) for 5 min. Cell growth was determined 48 h after incubation with the compounds. GI_{50} = 50% growth inhibition; TGI = total growth inhibition; LC_{50} = 50% lethal concentration; n = 4. Error bars represent standard deviation.

completely inhibited, has been determined to be 8.9 μM for **2**. Consequently, dabrafenib_photo (**2**) can be considered as an antiproliferative agent against $BRAF^{V600E}$-mutated melanoma cells *in vitro* although less potent than vemurafenib (TGI = 2.0 μM). Strikingly, the dose–response curve for dabrafenib (**1**) does not show the typical sigmoidal fit. Although **1** exhibits nanomolar cytostatic activity, in a higher concentration range between 1 and 30 μM the dose–response curve showed reproducibly unusual results with only weak inhibition of cell growth (Figure 4a). This unconventional cellular response at lower micromolar dabrafenib concentrations may indicate a special situation in SKMEL28 cells, e.g., efflux pump-mediated resistance, and should be explored in more detail in future studies.

The proliferation assays described above were repeated with the compound treated SKMEL28 cells exposed to UV light at 365 nm (5 min, 1.13 kW/m^2). The determined dose–response curves are shown in Figure 4b. As expected from our former studies,[8] there is no change in the cellular response to the reference inhibitor vemurafenib caused by irradiation. However, irradiated dabrafenib (**1**) shows a comparable dose–response curve to dabrafenib_photo (**2**) providing strong evidence for the photoinduced intracellular conversion of **1** to **2** *in vitro*.

To further prove our hypothesis of intracellular photo-induced transformation of dabrafenib (**1**) to its derivative **2**, we used the autofluorescence of **2** (Supplementary Figure S8b) and performed fluorescence microscopy experiments. First, the melanoma cells SKMEL28 were incubated with dabrafenib_-photo (**2**). The compound passed cellular membrane and could be clearly detected within the cells (Figure 5a). In contrast, dabrafenib (**1**) was not visible under the same fluorescent microscopic conditions (Figure 5b, second column left) because of its different excitation wavelength. Treating cells with dabrafenib (**1**) and exposure to increasing dosage of UV irradiation at 365 nm shows that photoinduced transformation of dabrafenib (**1**) to fluorescent **2** takes place (increasing fluorescence by enduring irradiation, Figure 5b). The control nuclei counterstaining with DAPI did not show any changes upon irradiation.

The combined staining and irradiation experiments displayed in Figure 5 provided strong evidence for the intracellular transformation of dabrafenib (**1**) to the novel compound **2** upon UV light exposure.

DOI: 10.1021/acsmedchemlett.6b00340
ACS Med. Chem. Lett. 2016, 7, 962–966

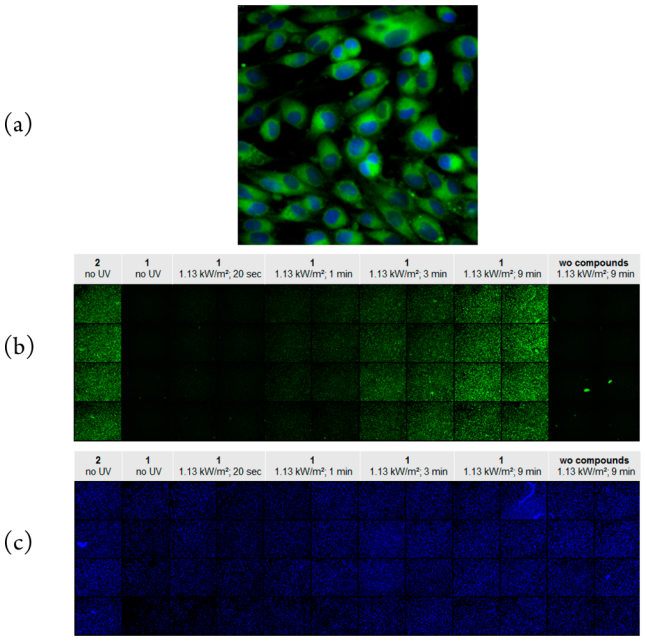

Figure 5. (a) SKMEL28 cells were incubated with dabrafenib_photo (**2**). The inhibitor was applied at 100 μM concentration and is shown in green. The cell nuclei were counterstained with 1 μg/mL DAPI and are marked in blue. The microscopic image was taken with 60× magnification. (b) SKMEL28 cells were seeded in 48 wells of a 96-well plate. The cells in the first column were incubated with dabrafenib_photo (**2**) without UV exposure. The cells in the columns 2 to 10 were incubated with dabrafenib (**1**) and exposed to increasing dosage of UV light at 365 nm (see captions above the columns). The cells in the last two right columns were not incubated with any compound but just irradiated with the highest UV amount. The overview image of the plate consists of single well images taken with 10× magnification. (c) The same cell plate from (b). All cell nuclei in the plate were counterstained with 1 μg/mL DAPI and are marked in blue.

To explore the cellular mechanism of action of dabrafenib_photo (**2**) in more detail, we sent compound **2** for the NCI 60 cell line screening[14] to the National Cancer Institute (NCI, Rockville, MD, USA). Herein, the cell growth of 59 different cancer cell lines was measured after incubation with 10 μM dabrafenib_photo (**2**). The determined one-dose mean graph is presented in the Supplementary Figure S12. Furthermore, we evaluated the data using the COMPARE Analysis tool.[15] Shortly, the cellular response to **2** was compared to cellular responses of 100 synthetic compounds in the NCI 60 database. The database compounds were then ranked in the order of similarity compared to dabrafenib_photo (**2**) assuming compound **2** may possess a similar mechanism of action to the compounds with high correlation coefficient in this ranking.[15] The results of the COMPARE analysis are shown in Supplementary Table S3. Strikingly, the first nine top-ranked entries are all either approved $BRAF^{V600E}$ inhibitors (dabrafenib and vemurafenib "Zelboraf") or 5-(2-substituted pyrimidin-4-yl)imidazo[2,1-*b*]thiazole derivatives (NSC: S755437, S755453, S761592, SS761584, S761586) previously described as antiproliferative agents against $BRAF^{V600E}$-mutated melanoma cell line A375.[16,13] Thus, the correlation results of the COMPARE analysis are further evidence that the novel compound **2** is an effective $BRAF^{V600E}$ inhibitor *in vitro*.

To summarize, we have revealed the photoinduced transformation of the approved kinase inhibitor dabrafenib (**1**) to a novel compound **2**. Dabrafenib solutions were evaluated to be instable upon exposure to both ultraviolet and daylight irradiation. This photoinduced degradation should be taken into account when handling dabrafenib solutions. The novel compound **2** was characterized as a $BRAF^{V600E}$ inhibitor *in vitro*. The enhanced autofluorescence of **2** could be used successfully for intracellular imaging of the inhibitor. The improved selectivity profile of **2** compared to dabrafenib (**1**) could be used as a starting point for development of more selective $BRAF^{V600E}$ inhibitors.

■ ASSOCIATED CONTENT

Supporting Information

The Supporting Information is available free of charge on the ACS Publications website at DOI: 10.1021/acsmedchemlett.6b00340.

Molecular modeling studies, chemical procedures, analytical data for the synthesis of **2**, irradiation experiments, kinase and cellular assays (PDF)

■ AUTHOR INFORMATION

Corresponding Author

*E-mail: cpeifer@pharmazie.uni-kiel.de. Tel: +49-431-880-1137.

Author Contributions

B.P. and C.P. conceived and designed the experiments. T.v.D. performed synthesis. V.O. performed photochemical characterization. B.P. performed the biological evaluation *in vitro* and wrote the paper.

Funding

This research project was supported by DFG (German Research Society) grant PE 1605/2-1.

Notes

The authors declare no competing financial interest.

■ ACKNOWLEDGMENTS

We thank Ulrich Girreser and Martin Schütt for excellent technical and analytical assistance at the Institute of Pharmacy in Kiel, Germany. We wish to thank the staff at the National Cancer Institute (NCI, Rockville, MD, USA) for NCI 60 profiling of **2**. We would like to thank the working group of Prof. Beitz at the Institute of Pharmacy in Kiel for providing us the DNA for gel electrophoresis.

■ ABBREVIATIONS

CHMP, Committee for Medicinal Products for Human Use; DAPI, 4′,6-diamidino-2-phenylindole; DMEM, Dulbecco's modified Eagle's medium; DMSO, dimethyl sulfoxide; DPBS, Dulbecco's phosphate buffered saline; FDA, Food and Drug Administration; HPLC, high performance liquid chromatography; LC, liquid chromatography; MS, mass spectrometry; NCI, National Cancer Institute; NSC, National Service Center; PBS, phosphate buffered saline; PFS, progression free; resp, respectively; UV, ultraviolet

■ REFERENCES

(1) Banzi, M.; De Blasio, S.; Lallas, A.; Longo, C.; Moscarella, E.; Alfano, R.; Argenziano, G. Dabrafenib: a new opportunity for the treatment of BRAF V600-positive melanoma. *OncoTargets Ther.* **2016**, *9*, 2725−2733.

(2) Rheault, T. R.; Stellwagen, J. C.; Adjabeng, G. M.; Hornberger, K. R.; Petrov, K. G.; Waterson, A. G.; Dickerson, S. H.; Mook, R. A., JR;

DOI: 10.1021/acsmedchemlett.6b00340
ACS Med. Chem. Lett. 2016, 7, 962−966

Laquerre, S. G.; King, A. J.; Rossanese, O. W.; Arnone, M. R.; Smitheman, K. N.; Kane-Carson, L. S.; Han, C.; Moorthy, G. S.; Moss, K. G.; Uehling, D. E. Discovery of Dabrafenib: A Selective Inhibitor of Raf Kinases with Antitumor Activity against B-Raf-Driven Tumors. *ACS Med. Chem. Lett.* **2013**, *4* (3), 358−362.

(3) Hauschild, A.; Grob, J.-J.; Demidov, L. V.; Jouary, T.; Gutzmer, R.; Millward, M.; Rutkowski, P.; Blank, C. U.; Miller, W. H.; Kaempgen, E.; Martín-Algarra, S.; Karaszewska, B.; Mauch, C.; Chiarion-Sileni, V.; Martin, A.-M.; Swann, S.; Haney, P.; Mirakhur, B.; Guckert, M. E.; Goodman, V.; Chapman, P. B. Dabrafenib in BRAF-mutated metastatic melanoma: A multicentre, open-label, phase 3 randomised controlled trial. *Lancet* **2012**, *380* (9839), 358−365.

(4) Sullivan, R. J.; Flaherty, K. T. Resistance to BRAF-targeted therapy in melanoma. *Eur. J. Cancer* **2013**, *49* (6), 1297−1304.

(5) Long, G. V.; Stroyakovskiy, D.; Gogas, H.; Levchenko, E.; de Braud, F.; Larkin, J.; Garbe, C.; Jouary, T.; Hauschild, A.; Grob, J. J.; Chiarion Sileni, V.; Lebbe, C.; Mandala, M.; Millward, M.; Arance, A.; Bondarenko, I.; Haanen; John, B. A. G.; Hansson, J.; Utikal, J.; Ferraresi, V.; Kovalenko, N.; Mohr, P.; Probachai, V.; Schadendorf, D.; Nathan, P.; Robert, C.; Ribas, A.; DeMarini, D. J.; Irani, J. G.; Casey, M.; Ouellet, D.; Martin, A.-M.; Le, N.; Patel, K.; Flaherty, K. Combined BRAF and MEK inhibition versus BRAF inhibition alone in melanoma. *N. Engl. J. Med.* **2014**, *371* (20), 1877−1888.

(6) Silas Inman. Dabrafenib/Trametinib Combination Approved for Advanced Melanoma. http://global.onclive.com/web-exclusives/FDA-Approves-First-Ever-Combination-for-Metastatic-Melanoma?p=2#sthash.qq6jAGJX.dpuf.

(7) Zhu, Z.; Liu, W.; Gotlieb, V. The rapidly evolving therapies for advanced melanoma–Towards immunotherapy, molecular targeted therapy, and beyond. *CR REV ONCOL-HEM* **2016**, *99*, 91−99.

(8) Horbert, R.; Pinchuk, B.; Davies, P.; Alessi, D.; Peifer, C. Photoactivatable Prodrugs of Antimelanoma Agent Vemurafenib. *ACS Chem. Biol.* **2015**, *10* (9), 2099−2107.

(9) Pinchuk, B.; Horbert, R.; Dobber, A.; Kuhl, L.; Peifer, C. Photoactivatable Caged Prodrugs of VEGFR-2 Kinase Inhibitors. *Molecules* **2016**, *21* (5), 570.

(10) Zindler, M.; Pinchuk, B.; Renn, C.; Horbert, R.; Dobber, A.; Peifer, C. Design, Synthesis, and Characterization of a Photoactivatable Caged Prodrug of Imatinib. *ChemMedChem* **2015**, *10* (8), 1335−1338.

(11) Committee for Medicinal Products for Human Use. *CHMP assessment report Tafinlar*. EMA/CHMP/242419/2013/corr 1, 2013.

(12) Laquerre, S.; Arnone, M.; Moss, K.; Yang, J.; Fisher, K.; Kane-Carson, L. S.; Smitheman, K.; Ward, J.; Heidrich, B.; Rheault, T.; Adjabeng, G.; Hornberger, K.; Stellwagen, J.; Waterson, A.; Han, C.; Mook, R. A.; Uehling, D.; King, A. J. Abstract B88: A selective Raf kinase inhibitor induces cell death and tumor regression of human cancer cell lines encoding B-RafV600E mutation. *Mol. Cancer Ther.* **2009**, *8*, B88−B88.

(13) Domingo, E.; Schwartz, S. BRAF (v-raf murine sarcoma viral oncogene homolog B1. *Atlas of Genetics and Cytogenetics in Oncology and Haematology [Online]* **2011**, DOI: 10.4267/2042/38125.

(14) Shoemaker, R. H. The NCI60 human tumour cell line anticancer drug screen. *Nat. Rev. Cancer* **2006**, *6* (10), 813−823.

(15) Paull, K. D.; Hamel, E.; Malspeis, L. COMPARE Introduction. Prediction of Biochemical Mechanism of Action from the In Vitro Antitumor Screen of the National Cancer Institute, 2015. https://dtp.cancer.gov/databases_tools/docs/compare/compare.htm (accessed August 15, 2016).

(16) Park, J.-H.; Oh, C.-H. Synthesis of New 6-(4-Fluorophenyl)-5-(2-substituted pyrimidin-4-yl)imidazo[2,1-b] thiazole Derivatives and their Antiproliferative Activity against Melanoma Cell Line. *Bull. Korean Chem. Soc.* **2010**, *31* (10), 2854−2860.

DOI: 10.1021/acsmedchemlett.6b00340
ACS Med. Chem. Lett. 2016, 7, 962−966